Materials Research. 2012; 15(6): 903-910
DOI: 10.1590/S1516-14392012005000113

Corrosion Behaviour of Al/SiC and Al/Al_2O_3 Nanocomposites

Tamer Samir Mahmoud[a]*, *El-Sayed Yousef El-Kady*[b], *Ayed Saad Merzen Al-Shihiri*[b]

[a]*Faculty of Engineering, King Khalid University – KKU, Abha, Kingdom of Saudi Arabia*
[b]*Faculty of Science, King Khalid University – KKU, Abha, Kingdom of Saudi Arabia*

Received: September 29, 2011; Revised: May 31, 2012

In the present investigation, the static immersion corrosion behavior of Al/Al_2O_3 and Al/SiC nanocomposites in 1 M HCl acidic solution was evaluated. The nanocomposites were fabricated using conventional powder metallurgy (P/M) route. The effect of nanoparticulates size and volume fraction on the corrosion behavior of nanocomposites was studied. The durations of the corrosion tests ranged from 24 to 120 hours and the temperatures of the solution ranged from ambient to 75 °C. The corrosion rates of the nanocomposites were calculated using the weight loss method. The results showed that both Al/SiC and Al/Al_2O_3 MMNCs have lower corrosion rates than the pure Al matrix. Such behavior was noticed at both ambient and higher temperatures. Generally, the Al/Al_2O_3 nanocomposites exhibited lower corrosion rates than the Al/SiC nanocomposites. The Al/Al_2O_3 (60 nm) nanocomposites exhibited the highest corrosion resistance among all the investigated nanocomposites. The corrosion rate was found to be reduced by increasing of the exposure time and the volume fraction of the nanoparticulates, while it was found to be increased by increasing of the nanoparticulates size and the solution temperature.

Keywords: *Nanocomposites, corrosion, aluminum alloys, powder metallurgy*

1. Introduction

Aluminum-based metal matrix composites (MMCs) become attractive for the automotive and aerospace industries when a lightweight and near-net-shape component is desired. Aluminum-based MMCs are well known for their high wear resistance, improved elevated temperatures tensile and fatigue strengths[1]. The mechanical and tribological characteristics of MMCs have been extensively studied, while corrosion characteristics are of increasing importance as MMCs become candidates for use in specific components subjected to corrosive media. Generally, the corrosion resistance of aluminum-based MMCs is less than the monolithic alloys, due to several reasons such as the crevices at the matrix/reinforcement interface, manufacturing defects, internal stress, microstructural differences and galvanic effects due to coupling of the matrix and reinforcement[2-4].

Recently, metal matrix nanocomposites (MMNCs) have become more attractive in various applications because of their improved mechanical properties over conventional micro-particle reinforced MMCs. These materials are expected to exhibit good corrosion resistance in the aggressive environments. Therefore, determination of the corrosion resistance of composite materials reinforced with nanoceramic additives is very important. Most studies conducted on Al matrix nanocomposites, have been focused on the corrosion susceptibility in NaCl solutions[5,6]. For example, El-Mahallawi et al.[5] studied the corrosion behavior in 3.5% NaCl solution of A356 Al alloy reinforced with nano- Al_2O_3 particulates. The results showed that the A356 the monolithic alloy exhibited high corrosion rates when compared with the nanocomposites. Durai et al.[6] studied effect of mechanical milling on the corrosion behavior of Al–Zn/Al_2O_3 composite in NaCl solution. Results of the corrosion tests, evaluated using the potentiodynamic method, indicate that corrosion of the investigated composite materials depends on the weight fraction of the reinforcing particles. The milled composite material Al–Zn/Al_2O_{3p} has higher corrosion resistance in the selected environment compared to unmilled composite Al–Zn/Al_2O_{3p}.

Literature regarding the corrosion behavior of Al matrix nanocomposites in acidic media is limited. Accordingly, the aim of the current investigation is to study the static immersion corrosion characteristics of Al/SiC and Al/Al_2O_3 nanocomposites in 1 M HCl solution. Several nanocomposites containing different sizes and volume fractions of SiC and Al_2O_3 nanoparticulates were prepared using conventional powder metallurgy (P/M) route.

2. Experimental Procedures

2.1. *Materials*

In the current study, commercially pure Al powder having minimum purity of 99.7% was used as a matrix material. The Al powders size ranged between 10 and 100 μm. Both of SiC and Al_2O_3 ceramic nanoparticulates were used as reinforcing agents. Each of SiC and Al_2O_3 nanoparticulates has two different average sizes, typically, 200 nm and 60 nm.

*e-mail: tsamir@benha-univ.edu.eg

2.2. *Fabrication of the nanocomposites*

Several Al-based nanocomposites containing up to 5 vol.% of SiC and Al_2O_3 nanoparticulates were prepared using conventional powder metallurgy (P/M) route as follows: Both Al powder and nanoparticulates in addition to 0.5-1.5 wt. (%) paraffin lubricant wax were placed into a blender, mechanically mixed until a homogeneous mixture is achieved, and then placed into containers. The mixed Al/nanoparticulates powders were cold compacted in a tool steel die shown schematically in Figure 1. The powders were then pressed using a hydraulic press havinga capacity of 400 kN. The compaction pressure applied was about 500 MPa. The nanocomposites produced from the cold compaction step were subjected to sintering at 600 °C for 100 minutes. The sintering process was performed under argon inert gas atmosphere. After sintering, the nanocomposites were subjected to hot extrusion. The nanocomposites billets were extruded at 500 °C using the extrusion die shown schematically in Figure 2. The heating process was carried out using Ni-Cr coils around the upper cylinder. The extrusion reduction ratio was 2 : 1 by area. The final nanocomposite samples had cylindrical shape of 10 mm diameter and about 100 mm length.

2.3. *Microstructural examinations*

Samples from the extruded rods were cut in transverse directions (i.e. cross sectional) for microstructural examinations. Specimens were ground under water on a rotating disc using silicon carbide abrasive discs of increasing grade up to 1200 grit. Then they were polished using 10 μm alumina paste and 3 μm diamond paste.

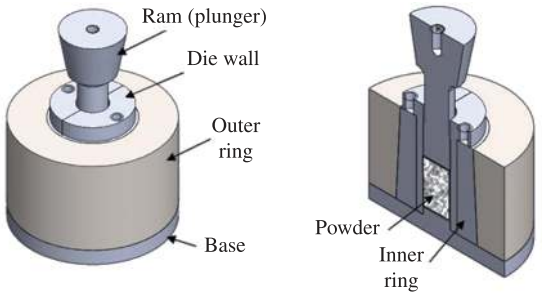

Figure 1. A schematic illustration of the cold compaction die.

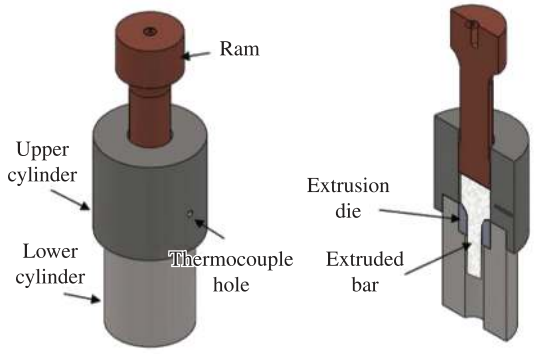

Figure 2. A schematic illustration of the extrusion dies.

Microstructural observations were conducted using optical and scanning electron microscopes.

2.4. *Static immersion corrosion tests*

The corrosion tests were static immersion tests conducted at ambient temperature, 50 and 75 °C using the conventional weight loss method to an accuracy of 0.1 mg. Each specimen was first weighed before being immersed in 100 mL of 1 M HCl solution and later taken out after 24, 48, 72, 96 and 120 hours respectively. After each corrosion test, the specimen was immersed in Clark's solution for 10 minutes and gently cleaned with a soft brush to remove adhered scales. Clark's solution is a standard mixture containing potassium chloride, potassium phthalate, potassium phosphate, boric acid and sodium hydroxide[7]. After drying thoroughly, the specimens were weighted again. The weight loss was measured and converted into corrosion rate expressed in mils penetration per year (mpy). The corroded surfaces were examined using scanning electron microscope (SEM).

Corrosion tests were carried out by suspending the disc-shaped samples (10 mm diameter and about 5 mm thick) in a still solution of 1 M HCl. To avoid crevice corrosion, the specimens were suspended in the solution with a plastic string. The results of corrosion tests were evaluated using weight loss measurements, performed following the ASTM-G31 recommended practice[8]. Before immersing in 1 M HCl solution, disc-shaped specimens were ground to 1200 grit and then cleaned with deionized water followed by rinsing with methanol and dried. For the accelerated tests, a 1 M HCl solution was prepared, and heated to 50 ± 2 and/or 75 ± 2 °C using an electric heater. The specimens were put into the warm solution and a glass cover was put on the top of the vessel to prevent evaporation.

3. Results and Discussion

3.1. *Microstructure of nanocomposites*

Figure 3 shows typical optical micrographs of the fabricated Al/Al_2O_3 and Al/SiC nanocomposites. It has been found that the agglomeration percent of the nanoparticulates tends to increase when the volume fraction of the nanoparticulates dispersed into the Al matrix is increased. Such agglomerations were found to be concentrated on the grain boundaries of Al grains (see Figure 3c). The agglomerations size was found varying between 1 and 5 μm. Generally, it has been found that the Al/Al_2O_3 nanocomposites exhibited better nanoparticulates distribution than Al/SiC nanocomposites. The Al/SiC nanocomposites exhibited more agglomeration percent when compared with the Al/Al_2O_3 nanocomposites. The agglomerations size in Al/SiC nanocomposites was found to vary between 0.5 and 10 μm. It has been found that the average size of the Al grains in the nanocomposites was not significantly influenced by the volume fraction and/or the size of nanoparticulates.

Figure 4 shows typical SEM micrographs for the investigated Al/Al_2O_3 and Al/SiC nanocomposites. It is clear that the nanoparticulates were successfully embedded in the Al matrix. According to the aforementioned results, it can

be concluded that the production of bulk nanocomposites using conventional P/M technique is effective. The SiC and Al_2O_3 nanoparticulates distribution in the Al matrix was fairly uniform. Although small agglomerates in Al/SiC and Al/Al_2O_3 nanocomposites still existed in the matrix, the agglomerates have been greatly improved when compared with the severe agglomerates in nanocomposites fabricated using traditional mechanical stirring method[9].

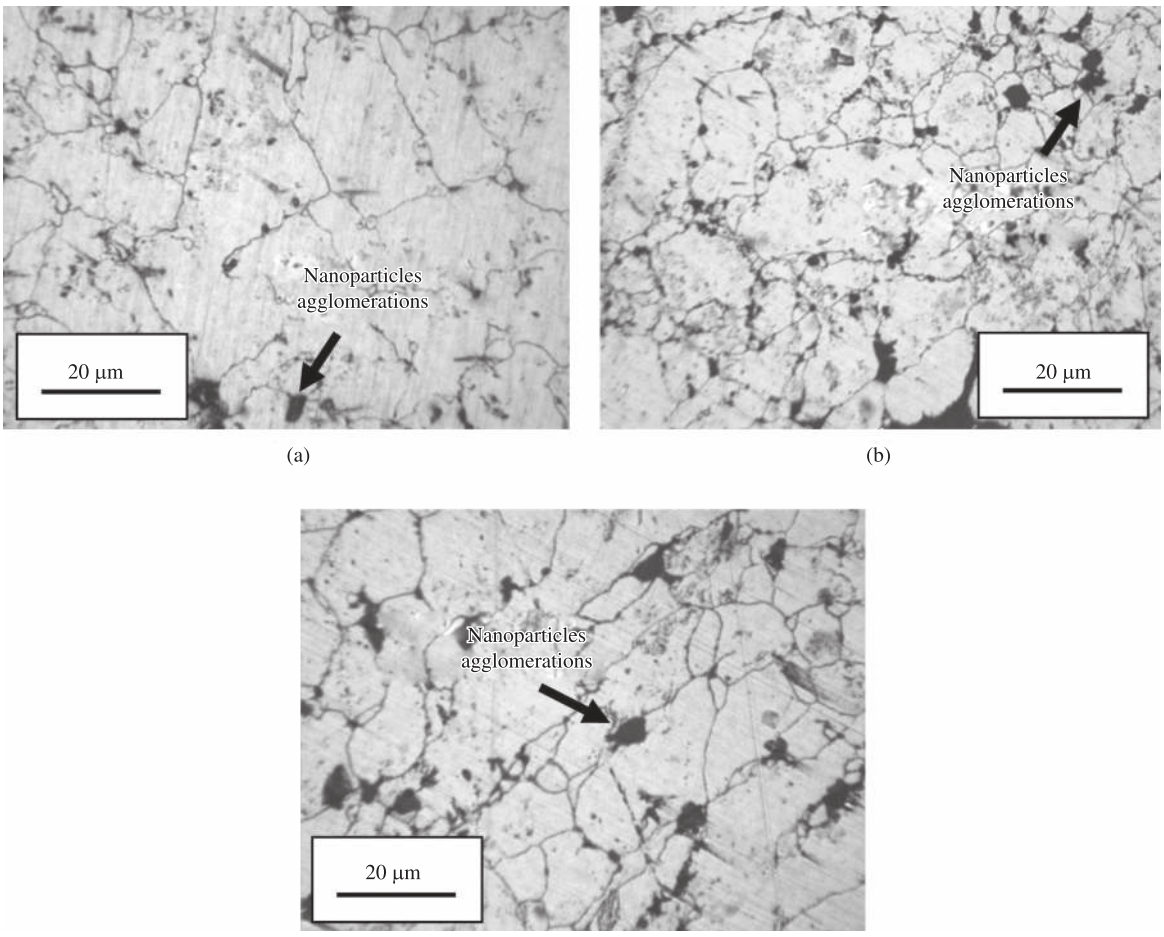

Figure 3. Optical micrographs of a) Al/3 vol.% Al_2O_3 (60 nm), b) Al/5 vol.% Al_2O_3 (60 nm) and c) Al/5 vol.%SiC (200 nm) nanocomposites.

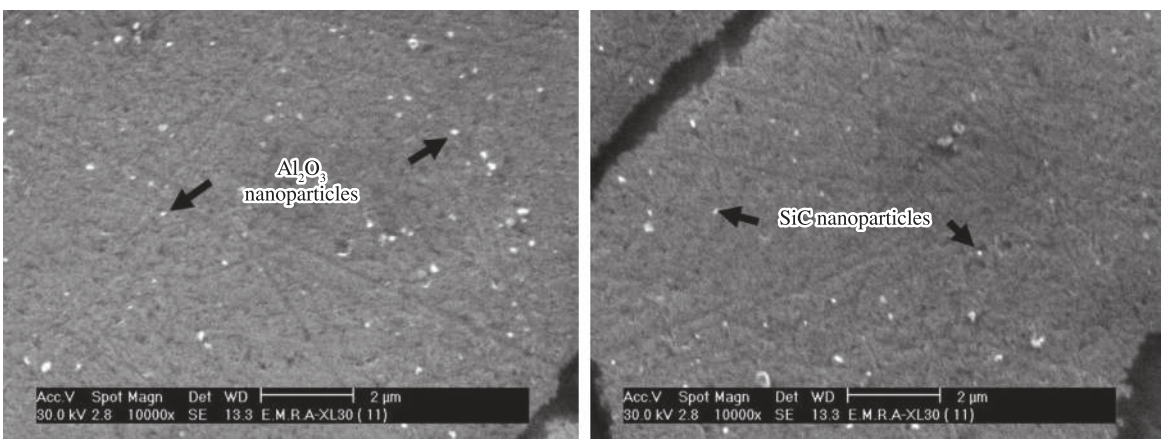

Figure 4. SEM micrographs of a) Al/3 vol.% Al_2O_3 (60 nm) and b) Al/3 vol.% SiC (200 nm) nanocomposites.

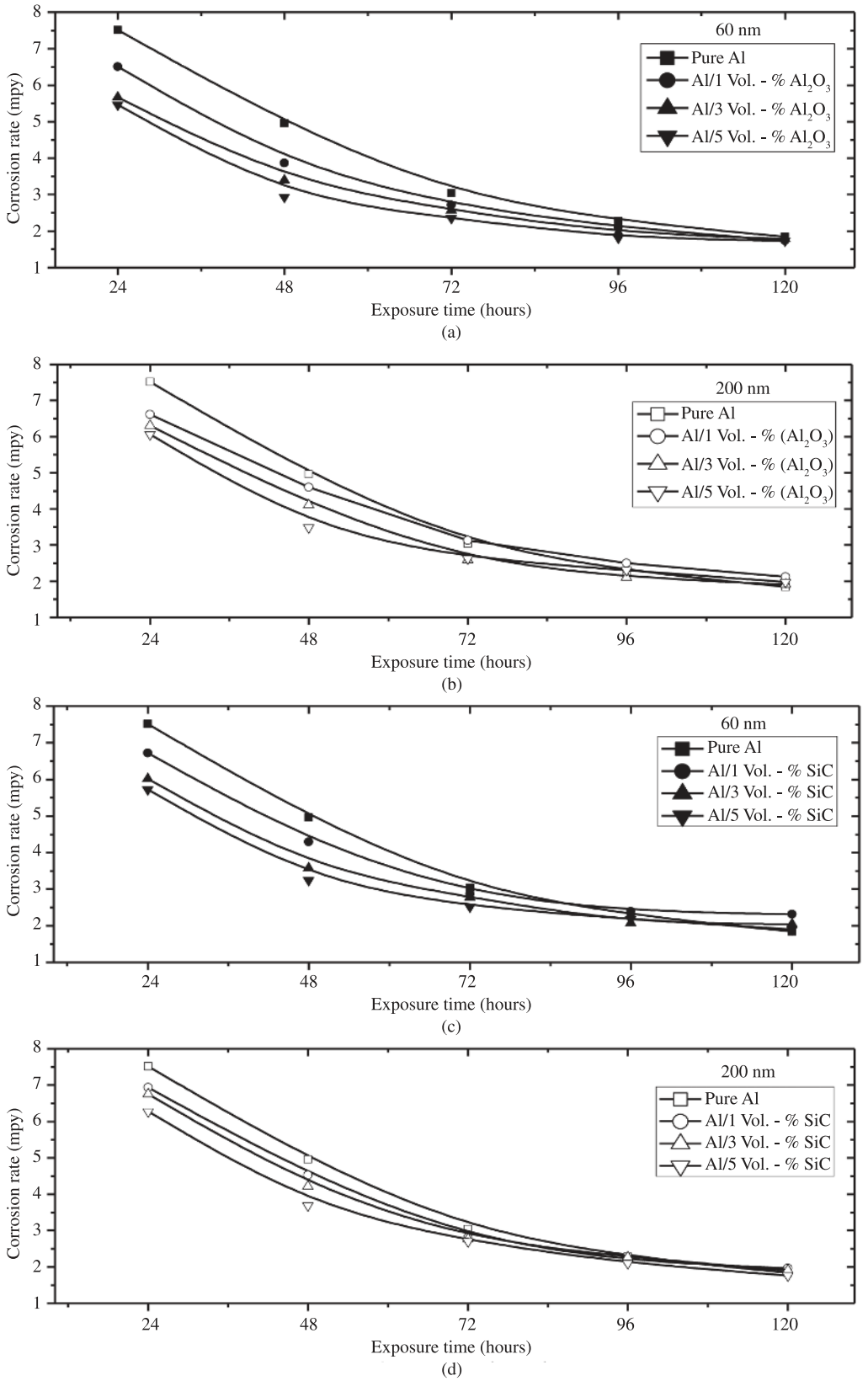

Figure 5. Variation of the corrosion rate with the exposure time in 1 M HCl at ambient temperature for nanocomposites reinforced with a) Al_2O_3 (60 nm); b) Al_2O_3 (200 nm); c) SiC (60 nm) and d) SiC (200 nm) nanoparticulates.

3.2. *Corrosion behavior of nanocomposites at ambient temperature*

Figure 5 shows the variation of the corrosion rate of Al/Al_2O_3 and Al/SiC nanocomposites with the exposure time in 1 M HCl at ambient temperature. The results showed that the corrosion rates of the nanocomposites decrease with increasing exposure time. Such observation implying that the corrosion resistance of the materials under investigation increases as the exposure time is increased. The phenomenon of decreasing the corrosion rate with respect to time indicates some passivation of the matrix alloy. For all the investigated nanocomposites, there is a trend of decreasing of the corrosion rate with the increase of the Al_2O_3 and SiC nanoparticulates volume fraction. The pure Al matrix exhibited higher corrosion rates than the Al/Al_2O_3 and Al/SiC nanocomposites. Both SiC and Al_2O_3 nanoparticulates are ceramic materials and they remain inert. It is expected that they are unaffected by the acid medium during the corrosion tests. The results revealed that corrosion rates of the Al/SiC and Al/Al_2O_3 nanocomposites were reduced by reducing the SiC and Al_2O_3 nanoparticulates size. Nanocomposites reinforced with 60 nm nanoparticulates exhibited lower corrosion rates than the nanocomposites reinforced with 200 nm nanoparticulates. Such notice was observed for both nanocomposites reinforced with both SiC and Al_2O_3 nanoparticulates. Moreover, the Al/Al_2O_3 nanocomposites exhibited lower corrosion rates than the Al/SiC nanocomposites.

From the aforementioned results, it can be concluded that both Al/Al_2O_3 and Al/SiC nanocomposites offer better corrosion resistance, in 1 M HCl solution, than the pure Al matrix. The corrosion behavior of nanocomposites depends on the type, size and volume fraction of the reinforcements.

3.3. *Effect of temperature on corrosion behavior of nanocomposites*

Figure 6 shows the variation of the corrosion rate of the Al/Al_2O_3 and Al/SiC nanocomposites with the temperature after exposure in 1 M HCl solution for 48 hours. It has been found that the nanocomposites have lower corrosion rates when compared with the pure Al matrix at elevated temperatures up to 75 °C. The corrosion rates of the pure Al as well as the nanocomposites were found to increase linearly with the temperature (see Figure 6). This effect may attribute to the increased diffusion rate of hydrogen with

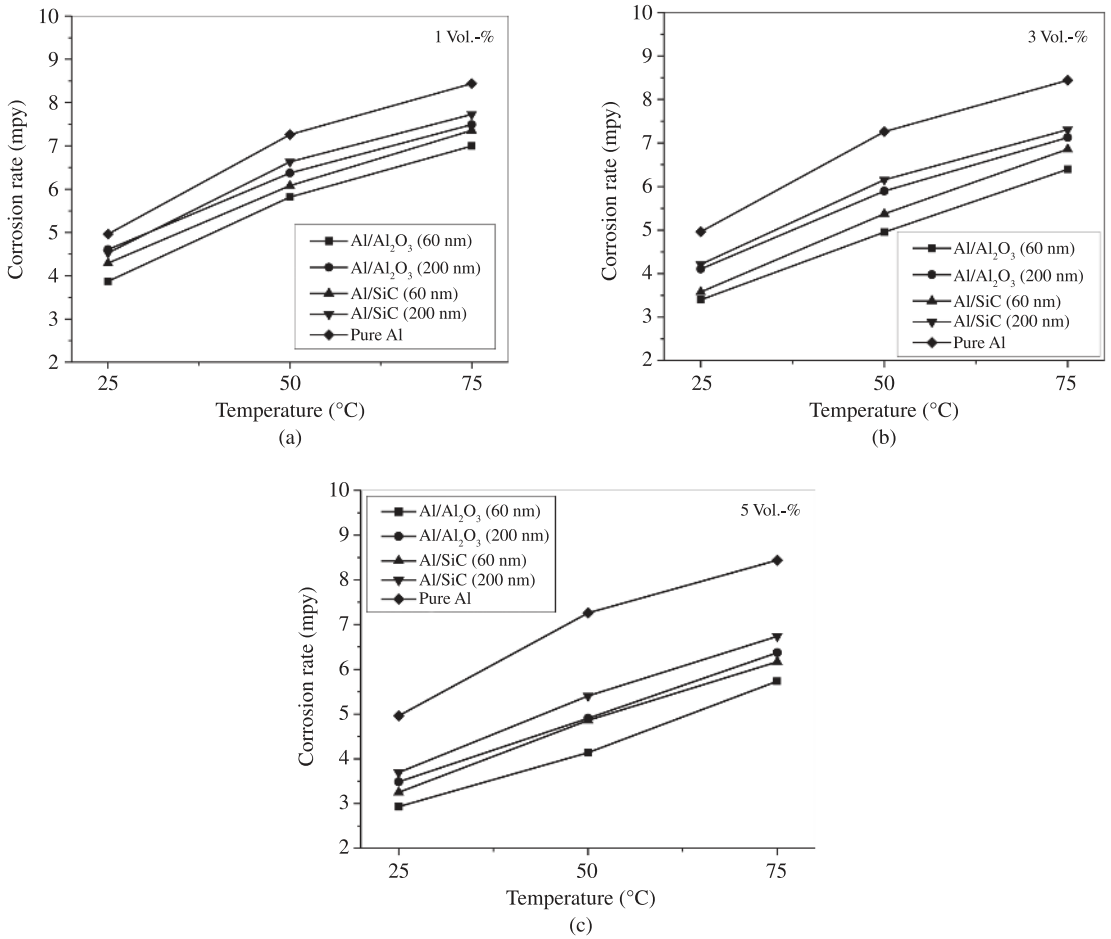

Figure 6. Variation of the corrosion rates with temperature for Al/SiC and Al_2O_3 nanocomposites containing a) 1 vol.%, b) 3 vol.% and c) 5 vol.% of nanoparticulates having average size of 60 and 200 nm.

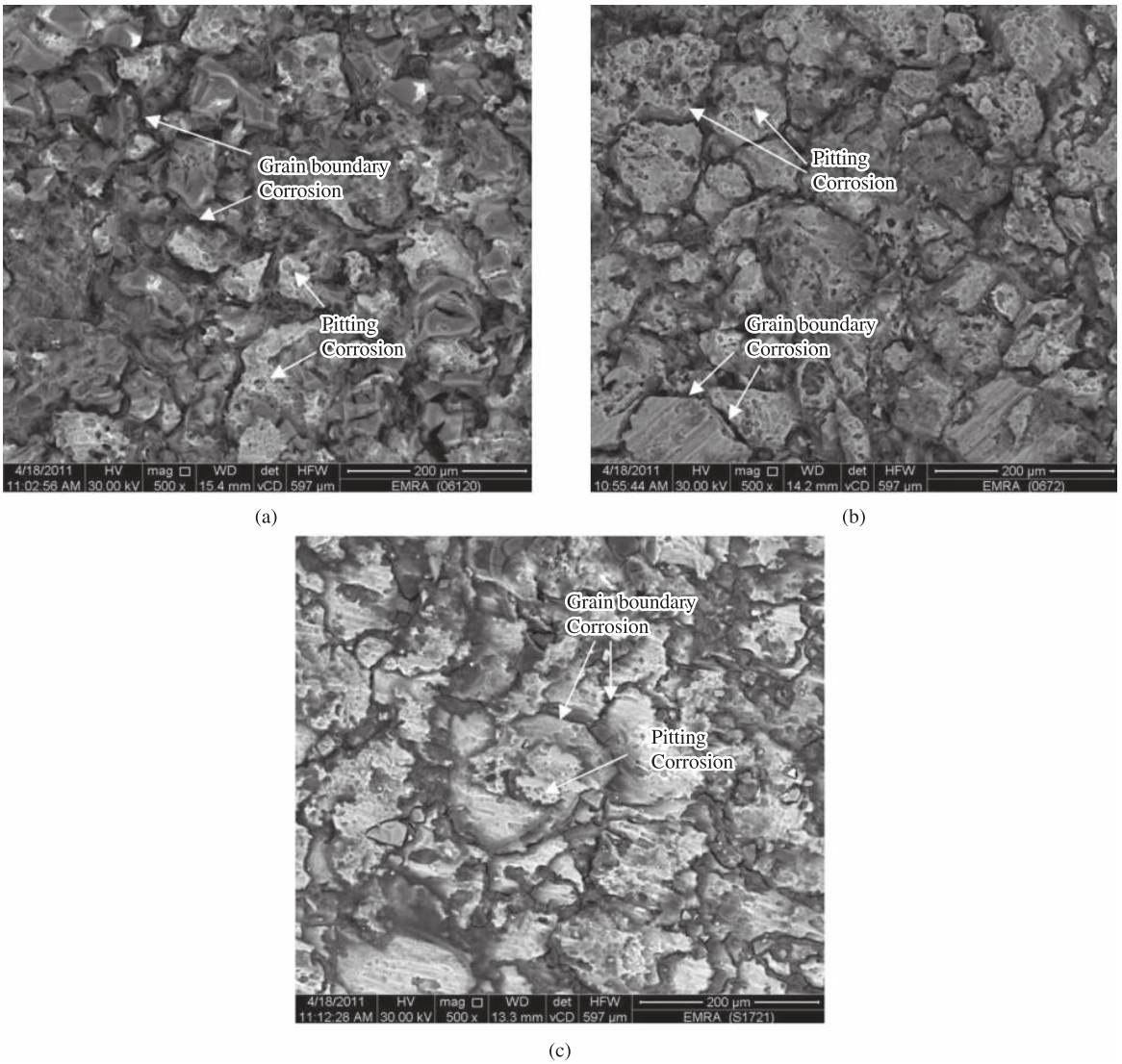

Figure 7. SEM micrographs of the corroded surfaces of a) pure Al matrix, b) Al/1 vol.%Al_2O_3 (60 nm) and c) Al/5 vol.%Al_2O_3 (60 nm) nanocomposites after exposure for 96 hours in 1 M HCl solution at ambient temperature.

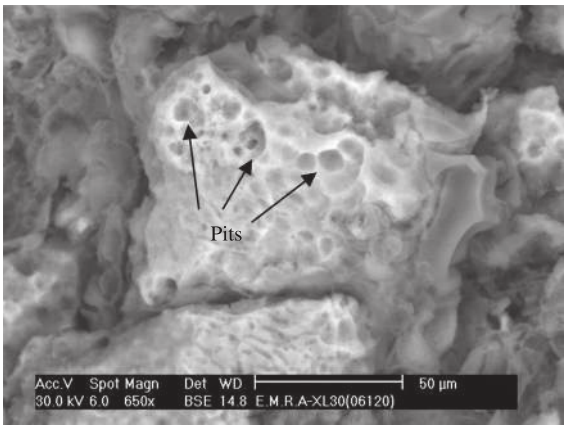

Figure 8. SEM micrograph shows the pitting corrosion occurred in 1 vol.% Al/Al_2O_3 (60 nm) nanocomposites after exposure for 96 hours in 1 M HCl solution at ambient temperature.

the increase in temperature, as well as the activation energy of the acid solution which boots hydrogen evaluation[10]. It has been found that, increasing the volume fraction and/or reducing the size of the nanoparticulates reduces the corrosion rate of the nanocomposites at both 50 °C and 75 °C. Such behavior was observed for both Al/SiC and Al/Al_2O_3 nanocomposites. However, the Al/Al_2O_3 nanocomposites exhibited lower corrosion rates than the Al/SiC nanocomposites. The Al/5 vol.% Al_2O_3 (60 nm) nanocomposites exhibited the lowest corrosion rates among all the investigated nanocomposites.

3.4. *Corrosion morphology*

Figure 7 shows typical SEM micrographs of the corroded surfaces of pure Al matrix and Al/Al_2O_3 nanocomposites, after exposure for 96 hours in 1 M HCl solution at ambient temperature. It is clear that the surface of the pure Al was severely damaged, especially at the grain

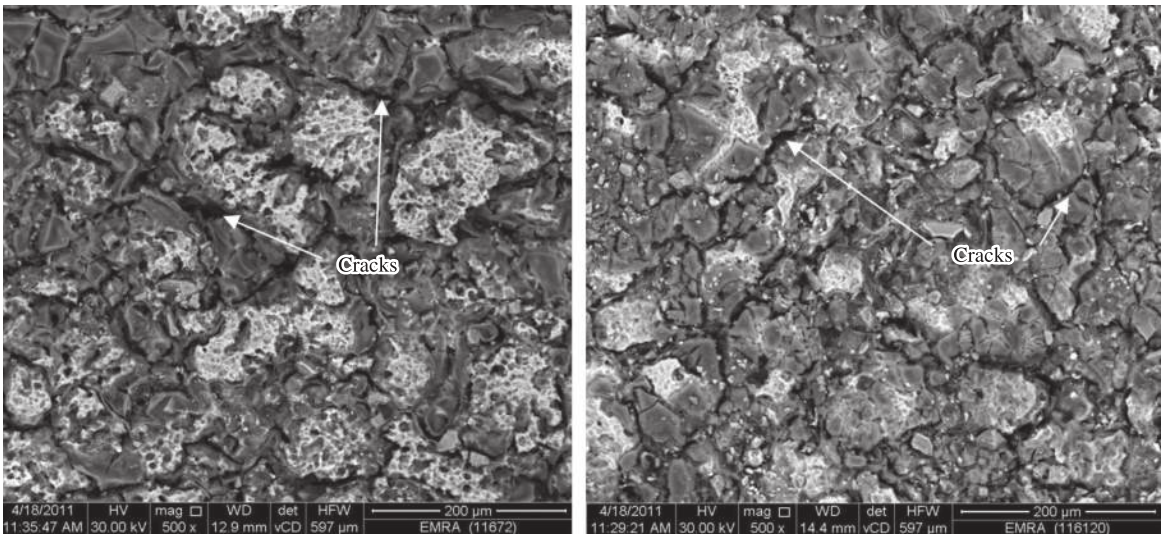

(a) (b)

Figure 9. SEM micrographs of the corroded surfaces of Al/SiC nanocomposites containing 1 vol.% of 200 nm SiC nanoparticulates after exposure in 1 M HCl solution for 96 hours at a) 50 and b) 75 °C.

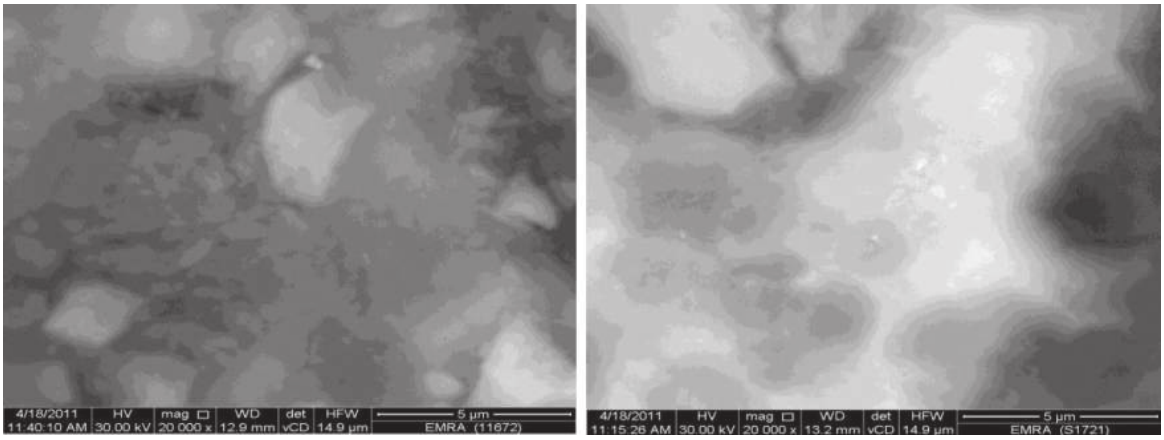

(a) (b)

Figure 10. High magnification SEM micrographs for the corroded surfaces of Al/SiC nanocomposite specimens after exposure in 1 M HCl solution for 96 hours at 50 °C, a) Al/1 vol.% SiC (60 nm); b) Al/1 vol.%SiC (200 nm).

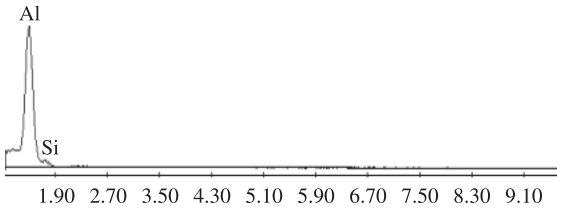

Figure 11. EDX analysis of SiC nanoparticulates located at the grain boundaries.

boundaries, when compared with the corroded surfaces of the Al/Al_2O_3 nanocomposites. Increasing the amount of Al_2O_3 nanoparticulates from 1 to 5 vol.% reduces the surface degradation (compare Figure 7b, c). In addition to grain boundary corrosion, pitting corrosion was observed in the pure Al matrix as well as the Al/Al_2O_3 and Al/SiC nanocomposites, especially those containing 1 vol% of nanoparticulates. Figure 8 shows typical corrosion pitting occurred in 1 vol.% Al/Al_2O_3 (60 nm) nanocomposites. It has been found that increasing the nanoparticulates volume fraction reduces the number of pits.

Typical SEM micrographs of the corroded surfaces of Al/SiC nanocomposites containing 1 vol.% of 200 nm SiC nanoparticulates after exposure in 1 M HCl solution for 96 hours at 50 and 75 °C are shown in Figure 9. It is clear that the amount of surface degradation increased with temperature. Surface crack were observed on the corroded surfaces at both 50 and 75 °C. The cracks were seen to develop along the grain boundaries. The size and depth of the cracks were found to increase with increasing both the exposure time and temperature.

Figure 10 shows typical SEM micrographs of the corroded surfaces of Al/SiC nanocomposites at the grain boundaries. The specimens were exposed to 1 M HCl solution at 50 °C for 96 hours. It has been found that the SiC nanoparticulates exist at the grain boundaries of the Al grains. Figure 11 shows EDX analysis of some SiC nanoparticulates located at the grain boundaries. It is important to mention that it was difficult to verify the SiC nanoparticulates from the SEM micrographs because of the low volume fraction and the small size of SiC nanoparticulates in the Al matrix.

The improvement of the corrosion resistance of Al matrix metal due to the addition of Al_2O_3 and SiC nanoparticulates may attribute to the fact that both SiC and Al_2O_3 are being ceramics and remain inert in the acid. They are hardly affected by the acidic medium. Although the corrosion rate of the nanocomposites is lesser than that of the Al matrix metal, the nanocomposites showed also the formation of pits on the surface. However, the number of pits gets decreased with the addition of SiC and Al_2O_3 nanoparticulates compared to that in the pure Al matrix metal. There is an evidence for the presence of grain boundary corrosion and pitting corrosion in the nanocomposites. This supports the effect of SiC and Al_2O_3 nanoparticulates in improving the corrosion resistance of the Al matrix metal. The SiC and Al_2O_3 nanoparticulates resist the severity of the acid attack to a certain extent. It is important to mention that there is hardly any information available in the literature about the corrosion behavior of the nanocomposites in acidic media.

4. Conclusions

According the results obtained from the current investigation, the following conclusions can be pointed out:

- The Al/SiC and Al/Al_2O_3 nanocomposites exhibited lower corrosion rates in 1 M HCl solution than the pure Al matrix. Such behavior was noticed at ambient and higher temperatures up to 75 °C;
- The Al/Al_2O_3 nanocomposites exhibited lower corrosion rates in 1 M HCl solution than the Al/SiC nanocomposites. The Al/Al_2O_3 (60 nm) exhibited the best corrosion resistance among all the investigated nanocomposites; and
- The corrosion rates of the Al/SiC and Al/Al_2O_3 nanocomposites in 1 M HCl solution were found to be reduced by increasing the exposure time and the volume fraction of the nanoparticulates, while increased by increasing the nanoparticulates size and the solution temperature.

Acknowledgements

This work is supported by the King Abdel-Aziz City of Science and Technology (KACST) through the Science and Technology Center at King Khalid University (KKU), Fund No. (NAN 08-173-07). The authors thank both KACST and KKU for their financial support. Special Thanks to Prof. Dr. Saeed Saber, Vice President of KKU, Dr. Ahmed Taher, Dean of the Scientific Research at KKU, and Dr. Khaled Al-Zailaie, Dean of the faculty of engineering at KKU, for their support.

References

1. ASM International. *ASM Handbook*. ASM; 2001. vol. 21, Composites.
2. Paciej RC and Agarwala VS. Metallurgical Variables Influencing the Corrosion Susceptibility of a Powder Metallurgy Aluminum/SiCw Composite. *Corrosion*. 1986; 42(12):718-729. http://dx.doi.org/10.5006/1.3583046
3. Shimizu Y, Nishimura T and Matsushima I. Corrosion resistance of Al-based metal matrix composites. *Materials Science and Engineering*: A. 1995; 198(1-2):113-118. http://dx.doi.org/10.1016/0921-5093(95)80065-3
4. Liu ZS, Huang B and Gu M. Corrosion behavior of Al/AlN_p composite in alkaline solution. *Materials Letters*. 2006; 60:2024-2028. http://dx.doi.org/10.1016/j.matlet.2005.12.149
5. El-Mahallawi IS, Eigenfield K, Kouta F, Hussein A, Mahmoud TS, Ragaie RM et al. Synthesis and Characterization of New Cast A356/$(Al_2O_3)_p$ Metal Matrix Nano-Composites. In: *Proceeding of the 2nd Multifunctional Nanocomposites & Nanomaterials*: International Conference & Exhibition; 2008; Sharm El Sheikh. ASME; 2008. http://dx.doi.org/10.1115/MN2008-47049
6. Durai T, Das Karabi and Das S. Effect of mechanical milling on the corrosion behavior of Al–Zn/Al_2O_3 composite in NaCl solution. *Journal of Materials Science*. 2007; 42:8209-8214. http://dx.doi.org/10.1007/s10853-007-1730-7
7. Bernad L, editor. *Hawk's Physiological Chemistry*. Reprint. New York: McGraw-Hill; 1976. p. 42.
8. American Society for Testing and Materials – ASTM. *ASTM G31–72*: Standard Practice for Laboratory Immersion Corrosion Testing of Metals. ASTM; 2004.
9. Lan J, Yang Y and Li XC. Microstructure and microhardness of SiC nanoparticulates reinforced magnesium composites fabricated by ultrasonic method. *Materials Science and Engineering*: A. 2004; 386:284-290. http://dx.doi.org/10.1016/j.msea.2004.07.024
10. Seah KHW, Krishna M, Vijayalakshmi VT and Uchil J. Effects of the temperature and reinforcement content on corrosion characteristics of LM13/Albite composites. *Corrosion Science*. 2002; 44:761-772. http://dx.doi.org/10.1016/S0010-938X(01)00074-9